AJNR

The Effect of Age on Odor-Stimulated Functional MR Imaging

David M. Yousem, Joseph A. Maldjian, Thomas Hummel, David C. Alsop, Rena J. Geckle, Michael A. Kraut and Richard L. Doty

AJNR Am J Neuroradiol 1999, 20 (4) 600-608
http://www.ajnr.org/content/20/4/600

AJNR Am J Neuroradiol 20:600–608, April 1999

The Effect of Age on Odor-Stimulated Functional MR Imaging

David M. Yousem, Joseph A. Maldjian, Thomas Hummel, David C. Alsop, Rena J. Geckle, Michael A. Kraut, and Richard L. Doty

BACKGROUND AND PURPOSE: **The effects of age, sex, and handedness on olfaction have not been adequately addressed with odor-stimulated functional MR imaging studies. We sought to determine the effect of age on functional MR imaging experiments performed with odor stimulation.**

METHODS: **Five right-handed subjects with a mean age of 73 years and five right-handed subjects with a mean age of 24 years underwent gradient-echo echo-planar functional MR imaging using binasal olfactory stimulation. Imaging parameters included 3000/30 (TR/TE) and a 5-mm section thickness in a 6-minute sequence with 30 seconds of pulsed odorants alternating with 30 seconds of room air. The data were normalized to a standard atlas, and individual and group statistical parametric maps (SPMs) were generated for each task. The SPMs were thresholded for a $P < .01$, and the volumes of activation and distribution of cluster maxima were compared for the two groups.**

RESULTS: **Analysis of the group SPMs revealed activated voxels in the frontal lobes, perisylvian regions, and cingulate gyri, with greater volume in the younger group than in the older group. The right inferior frontal, right perisylvian, and right and left cingulum had the largest number of voxels activated. The most common sites of activation on individual maps in both groups were the right inferior frontal regions and the right and left superior frontal and perisylvian zones.**

CONCLUSION: **Given similar olfactory task paradigms, younger subjects showed a greater number of activated voxels than did older subjects. One must be cognizant of this effect when designing studies of odor-stimulated functional MR imaging.**

The effects of age, sex, and handedness on olfaction have not been adequately addressed with odor-stimulated functional MR imaging studies (1–6). These factors are known to have strong influences on the results of psychophysical tests of olfaction (7–10). In general, women tend to score higher than men on tests of odor identification and odor detection in all age groups (11–13). This applies across many ethnic groups (8). There may be an effect of estrogen as well, since premenopausal and postmenopausal women perform differently (14). How much of a factor age plays beyond the hormonal effects is difficult to determine, but it is true that the elderly identify and detect odors less well than the young (10, 15, 16). On the University of Pennsylvania Smell Identification Test (UPSIT), peak performance usually occurs in the third through fifth decades and declines so markedly after the seventh decade that many individuals are functionally severely microsmic if not anosmic (7, 13).

We sought to ascertain whether subjects over 60 years of age would show the same decline in function on odor-stimulated functional MR imaging studies that is present on psychophysical tests of odor detection and odor identification (10, 13). We hypothesized that the functional MR imaging correlate would be a diminution in the activated volume in subjects over the age of 60 compared with those in the under-40 age group.

Methods

All subjects were initially screened for any possible causes of smell dysfunction before being invited to enter the study.

Received September 30, 1998; accepted after revision December 9.

Supported by research grant 5 PO1 DC 00161-15 from the National Institute on Deafness and Other Communication Disorders, National Institutes of Health.

From the Department of Radiology (D.M.Y., J.A.M., D.C.A., R.J.G.) and the Smell and Taste Center (D.M.Y., T.H., R.J.G., R.L.D.), University of Pennsylvania Medical Center, Philadelphia; and the Department of Radiology, Johns Hopkins Hospital, Baltimore, MD (D.M.Y., M.A.K.).

Address reprint requests to David M. Yousem, MD, Department of Radiology, Johns Hopkins Hospital, 600 N Wolfe St/Houck B-112, Baltimore, MD 21287.

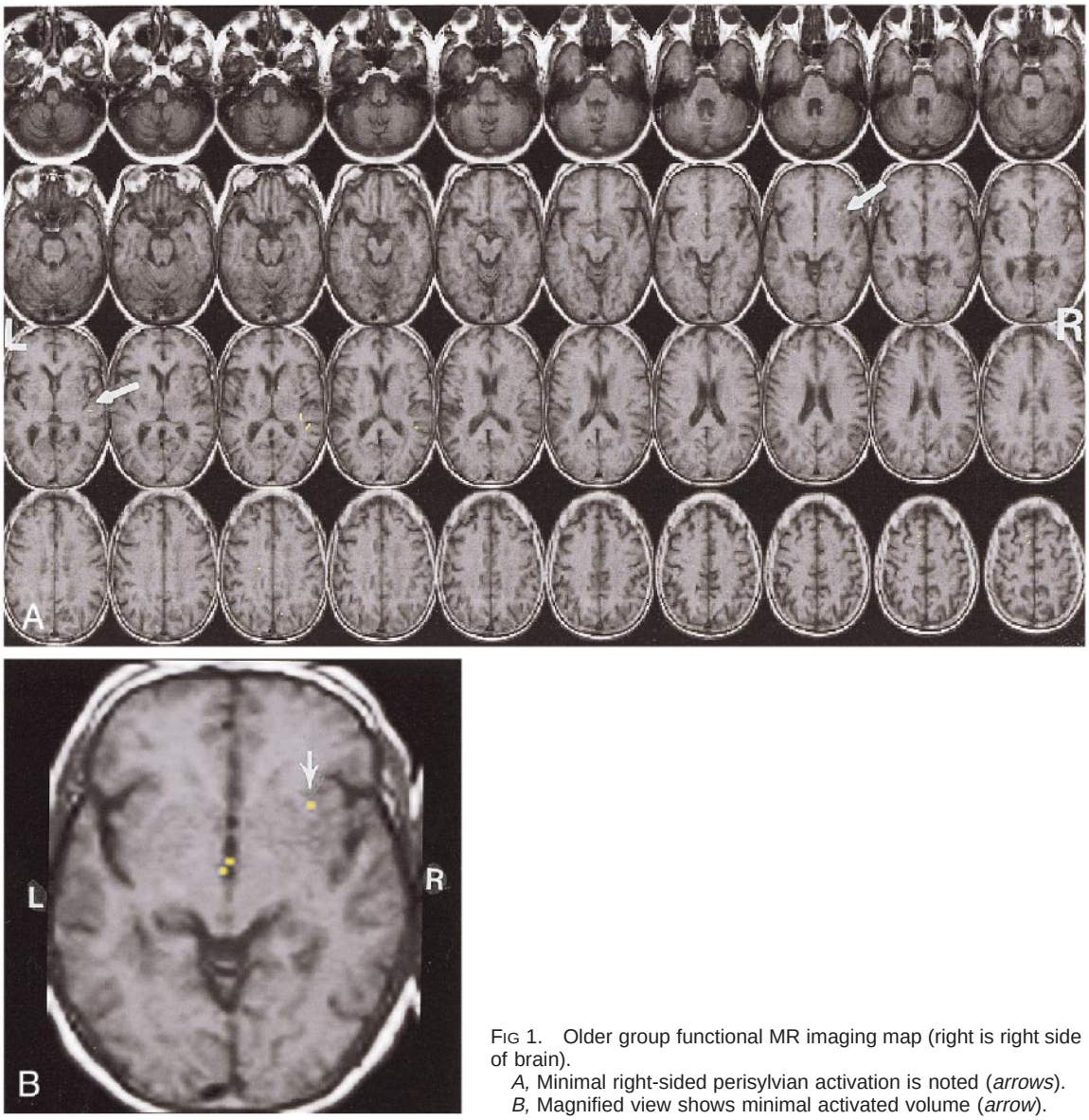

FIG 1. Older group functional MR imaging map (right is right side of brain).
A, Minimal right-sided perisylvian activation is noted (*arrows*).
B, Magnified view shows minimal activated volume (*arrow*).

Individuals who smoked, had a history of head trauma, were on medications that could affect their sense of smell, or had any olfactory or gustatory complaints were excluded. All subjects reported a normal sense of smell. The young subjects were recruited from employees at the Hospital of the University of Pennsylvania. The older subjects were recruited from the Veterans Administration of Philadelphia Volunteer Registry and through advertising in local publications.

After the subjects gave informed consent (approved by the institutional review board at our institution), they completed a standardized survey to assess handedness (17). All subjects also underwent odor identification testing with the 40-item UP SIT (20 items each nostril) (7, 10, 18).

There were five right-handed subjects (three women and two men) ranging in age from 62 to 80 years (mean age, 73 years; SD, 7.9) who made up the older-aged group. These subjects were compared with three right-handed women and two right-handed men, 18 to 27 years old (mean age, 24 years; SD, 3.3). The older group had a mean UPSIT score of 33 out of 40 (SD = 5.8) and the younger group had a mean UPSIT score of 38 (SD = 2.0). These values fall within the range of normal for their age groups (13). The individuals of both age groups also underwent the standard minimental status examination and scored within the normal range.

Imaging was performed on a 1.5-T scanner equipped with a GE Horizon Echospeed system (Signa; GE Medical Systems, Milwaukee, WI) for echo-planar imaging. Foam cushions were used to immobilize the head within the coil to minimize motion degradation. Localization for the functional MR imaging studies consisted of a sagittal T1-weighted (500/11/1 [TR/TE/excitations]) image followed by axial T1-weighted (500/11/1) 5-mm interleaved images with a matrix of 192 × 256 through the entire brain. The conventional T1-weighted axial images were used both as anatomic templates on which to overlay functional data and for normalization to a standard Talairach atlas. An echo-planar chemical-shift imaging data set was then obtained to be used to correct for spatial shifts and distortions on the echo-planar images, which can lead to misalignment with the T1-weighted anatomic images.

Functional MR studies were performed in the axial plane using multisection gradient-echo echo-planar imaging. Scan parameters included a 64 × 40 matrix, 24 × 15-cm field of view, 3000/30/1, 5-mm thickness, and a 90° flip angle, delivering a voxel resolution of approximately 4 × 4 × 5 mm. The

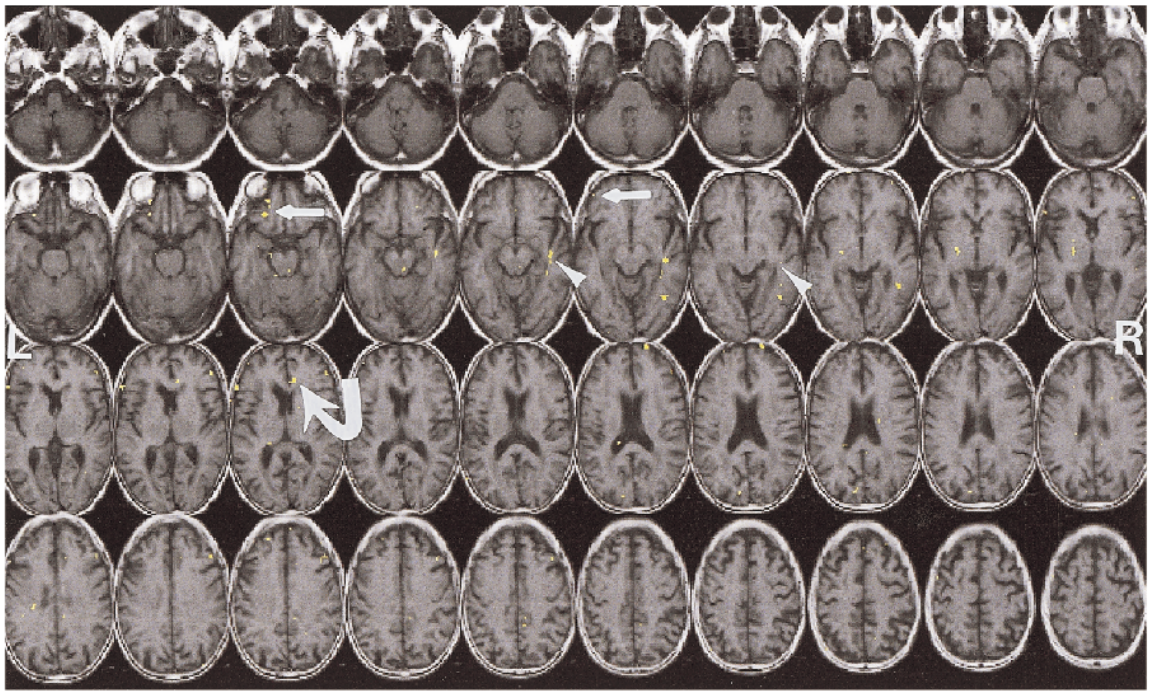

FIG 2. Activation map in single older subject. Left inferior frontal (*straight arrows*), right perisylvian (*arrowheads*), and right cingulate (*curved arrow*) areas show activation.

TE of 30 was lowered from a standard 50- to 60-millisecond value used in other functional MR imaging experiments in an attempt to optimize visualization of the inferomedial temporal and orbitofrontal regions. In total, 120 images were acquired at each of 24 section locations per run during the course of a 6-minute functional MR scan. Each task paradigm consisted of alternating rest-stimulus cycles (30 seconds each) during the 6-minute scan. We used stimulants (eugenol, phenyl ethyl alcohol, or phenyl ethyl alcohol alternating with hydrogen sulfide) that were selective for olfactory nerve stimulation in the nose. These odorants are rarely detected by anosmics (who cannot detect olfactory nerve stimulants but can detect trigeminal nerve stimulants) (9, 19). Subjects who have been trained to detect trigeminal stimulation in the nose have confirmed the lack of trigeminal stimulation by these odorants (9, 19).

Olfactory stimuli were delivered to the subjects by using a Burghart OM4-B olfactometer (Wedel, Germany) with continuous air flow (4 L/min). This machine delivered the stimulants through tubing to a nose piece inserted into the subjects' nostrils that was similar in size to oxygen nasal cannula tubing; however, the air flow and humidity were precisely regulated (20). Odors were delivered to both nostrils for 1 second every 4 seconds during the 30-second ''on period.'' During the 30-second ''off period'' the subject received humidified and filtered room air at the same flow rate. Between the pulsed odorants during the on period, humidified and filtered room air was also administered (eg, 1 second of odorant then 3 seconds of room air for seven cycles followed by 30 seconds of continuous room air, repeated six times). By pulsing the odorants we sought to decrease the chance of habituation. The olfactometer, which is also used for olfactory event related potential measurements, has been precisely calibrated to afford sharp on-off periods (measured in milliseconds) with no retention of odors in the specially designed tubing.

During the functional MR imaging sequences, the subjects were told to breathe normally (no change in respiratory rates) without sniffing (21) and to concentrate on the odors. They were not asked to identify the odors nor were they told what the odors were. The room was dark with no other stimulation besides the odorants. After the functional MR imaging experiment, the subjects were asked to tell what the odor smelled like to them, to rate its intensity, and to judge its pleasantness. In none of the cases was the odor judged to be below a 5 rating on a 10-point rating scale of 0 (no smell) versus 1 (barely detectable) to 10 (very strong). All subjects detected the odors.

The functional MR imaging raw echo amplitudes were saved and transferred to a Sun Ultrasparc 1 (Sun Microsystems, Mountain View, CA) for off-line reconstruction using in-house software developed in IDL (Research Systems Inc, Boulder CO). Correction for image distortion and alternate k-space line errors was performed on each image on the basis of data acquired during phase-encoded reference imaging. Statistical parametric maps (SPMs) were generated using SPM96 (22–25) (from Wellcome, Cognitive Neurology, London, UK) implemented in Matlab (Mathworks Inc, Sherborn, MA), with an IDL interface. The IDL interface was developed in-house in collaboration with the UMDNJ (Newark, NJ) functional MR imaging lab. The T1-weighted images were normalized to a standard atlas (Talairach space). The functional data sets were motion corrected (intrarun realignment) within SPM96 using first- and second-order motion correction, as well as a first-order correction for spin history, using the first image as the reference (26, 27). The six parameters of this rigid-body transformation were estimated by using a least-squares approach (25), which is based on an approximate linear relationship between the images and their partial derivatives with respect to parameters of the transformation. The transformation is computed in three dimensions. In addition, the spin-history correction employed removes any movement-related confounds according to an arma-like model of these effects. This algorithm achieves accurate subvoxel registration. In addition, we performed a second 3D rigid-body realignment (interrun realignment) to correct for motion between successive runs. The functional data sets were normalized to Talairach space using image header information to determine the 16-parameter affine transform between the functional data sets and the T1-weighted images in combination with the transform computed within SPM96 for the T1-weighted anatomic images to Talairach space. The normalized data sets were resampled to $4 \times 4 \times$

TABLE 1: Number of voxels activated in each region by subject group (*P* value set at .01)

Subject Group	RIF	LIF	RIMT	LIMT	RPS	LPS	RC	LC	RSF	LSF
Younger men and women	12	0	0	0	12	4	11	18	3	4
Older men and women	1	0	0	0	9	0	0	0	3	1

Note.—RIF indicates right inferior frontal; LIF, left inferior frontal; RIMT, right inferomedial temporal lobe; LIMT, left inferomedial temporal lobe; RPS, right perisylvian; LPS, left perisylvian; RC, right cingulate; LC, left cingulate; RSF, right superior frontal; LSF, left superior frontal.

TABLE 2: Sites of activation in Talairach space in younger and older subjects

	RIF	RPS	LPS	RC	LC	RSF	LSF
Younger subjects							
Talairach coordinates identified in group maps in these sites (*X*, *Y*, *Z*)	24, 52, 10 32, 40, 15	20, 24, −4 36, 24, −4 32, 28, −9 56, −19, 20 48, 24, 10	−51, −7, 10 −31, −19, 15	8, 36, 0 12, −31, 25	−7, 20, 35	24, 48, 25	
Older subjects							
Talairach coordinates identified in group maps in these sites (*X*, *Y*, *Z*)	24, 56, 5	48, −3, 5 48, −23, 0				48, 12, 30	−31, 44, 25

Note.—RIF indicates right inferior frontal; RPS, right perisylvian; LPS, left perisylvian; RC, right cingulate; LC, left cingulate; RSF, right sup erior frontal; LSF, left superior frontal.

5 mm within Talairach space using sinc interpolation. The data sets were smoothed using an 8 × 8 × 10-mm full width at half-maximum gaussian smoothing kernel, and SPMs were generated using the general linear model within SPM96 (25, 27). A 6-second time-shifted boxcar waveform was used as the reference paradigm, and the ANCOVA model with global activity as a confound was used for the statistical analysis. In addition, high-pass and low-pass filters were used as confounds within the analysis. The resulting set of images represents SPMs of the *t* statistic SPM{*t*}. Individual SPMs were generated for every run for each subject. The SPM{*t*} was transformed to the unit normal distribution SPM{*Z*} and thresholded at $P < .05$. Group SPMs were also constructed across subjects for each condition using the smoothed normalized data sets. The group SPMs were thresholded for $P < .01$. The thresholded SPMs were overlaid onto the anatomic normalized images for display within IDL.

Quantitative analysis was performed for each group-averaged and individual map and the number of voxels activated was computed for the right and left inferior and superior frontal lobes, the right and left perisylvian regions, the right and left inferomedial temporal lobes, and the right and left cingulate gyri. These regions were defined using standard neuroanatomic landmarks. The superior and posterior margins of the sylvian fissures were used as the boundaries for the temporal lobe, and the central sulcus posteriorly and sylvian fissure inferiorly were used to delineate the frontal lobe. The inferior frontal lobe was defined as that portion of the frontal lobe below the genu of the corpus callosum in the Talairach maps. The inferior frontal lobe included the orbitofrontal, frontopolar, and gyrus rectus regions. The perisylvian region included the insula and the regions of the temporal lobe bounded by the sylvian fissure. The inferomedial temporal lobe was defined as the region that was located inferior and medial to the temporal horns of the lateral ventricles. This region included the entorhinal and piriform cortices as well as the hippocampus and parahippocampus.

The group and individual maps were analyzed by two neuroradiologists (DMY, JAM) in a consensus reading. A third neuroradiologist (MAK) from another institution who was not involved in the functional MR imaging studies then independently reviewed the composite maps of the older and younger groups in order to assign locations of activated voxels based on the anatomic description given in the paragraph above. The assignment of voxels between the independent reviewer and the consensus interpretation was in agreement in 62 (83%) of 75 instances. Of the 13 discrepancies, seven involved the differentiation between inferior and superior frontal lobes (the genu of the corpus callosum could be seen on three separate images), four were referable to the difference between the perisylvian versus frontal opercular (superior frontal) regions, and two were based on the location of the superior cingulum versus superior frontal regions. Twelve localization discrepancies occurred in the younger subjects' group map and one in the older subjects' map. For the purpose of the results, the consensus readings of the two neuroradiologists from the home institution are reported.

Results

On the group SPMs, the older subjects showed the largest number of activated voxels (n = 9) in the right perisylvian region, followed by the right superior frontal region (n = 3) (Fig 1A and B). Single voxels of activation were noted in the right inferior frontal and left superior frontal zones (Table 1). The Talairach coordinates for the sites of activation are depicted in Table 2. Despite this relative paucity of activation on group-averaged maps, the individual maps showed activation in most subjects in the right perisylvian, right and left superior frontal, and right and left inferior frontal regions (Fig 2, Table 3). There was a right-sided

TABLE 3: Number of subjects who had activated voxels in each area (*P* value set at .05)

Subject Group	RIF	LIF	RIMT	LIMT	RPS	LPS	RC	LC	RSF	LSF
Younger men and women	5	2	2	2	4	5	4	1	4	4
Older men and women	4	3	1	2	5	3	2	1	4	4

Note.—RIF indicates right inferior frontal; LIF, left inferior frontal; RIMT, right inferomedial temporal lobe; LIMT, left inferomedial temporal lobe; RPS, right perisylvian; LPS, left perisylvian; RC, right cingulate; LC, left cingulate; RSF, right superior frontal; LSF, left superior frontal.

preponderance of activation across all these regions, even on the individual maps.

The younger subject group showed greater volumes of activation in all sites on the group SPMs (Fig 3A and B). The sites of greatest activation identified in the older group (the right perisylvian, right superior frontal, right inferior frontal, and left superior frontal regions) were also activated to the greatest degree in the younger group (Table 1), though in different absolute Talairach coordinates (Table 2). In addition, the group maps of the younger subjects showed activation in the left superior frontal, left perisylvian, and both cingulate regions. All five young subjects showed activation in the right inferior frontal and left perisylvian regions (Fig 4, Table 3).

While there were areas of activation in the parietal and occipital regions in the younger subjects' group maps, these were believed to represent either visual stimulation artifacts (occipital), statistical noise, or supplemental sensory areas (parietal). These activated voxels were not selectively evaluated, since they did not occur in the older subjects' group maps.

Discussion

The olfactory system has rarely been a subject of analysis in the imaging literature. While smells are perceived in the upper nasal cavity by olfactory neuroepithelial receptors, the primary olfactory nerves pierce the cribriform plate to stimulate and synapse with olfactory bulb nuclei. From the olfactory bulb and tract, fibers pass in the olfactory stria to septal nuclei at the base of the brain just inferior and anterior to the rostrum of the corpus callosum. From the medial and lateral septal nuclei, fibers extend to the limbic system with branches to the uncus, hippocampus, parahippocampal region, septum pellucidum, fornices, amygdala, and gyrus rectus regions. Additional connections are made to the orbitofrontal, superior frontal, and perisylvian regions for higher-order odor processing.

Most functional imaging studies at rest and with activity have tended to include only younger subjects (28–31). Within the limited age range of the subjects (19–38 years) Andreason et al (31) and Miura et al (32) found no age differences in regional and global glucose metabolic rates among subjects studied with positron emission tomography (PET). However Azari's group (33) noted an age-related reduction in frontal and parietal metabolic rates for glucose in the resting state when women less than 40 years old were compared with those over 64 years old.

During visual processing of faces and location, older subjects have shown less activation than younger subjects in the extrastriate cortex, but the older subjects had larger blood flow increases to the occipitotemporal cortices (34). During visually guided location matching, the older subjects actually showed greater activation than younger subjects in the prefrontal and parietal cortices (34). The authors suggest that older subjects recruit more areas of the brain to process visual data than younger subjects do in order to compensate for less occipital activation (34).

Ross et al (35) examined the effect of age on functional MR imaging results when the subjects underwent 8 Hz of photic stimulation. Nine elderly subjects (mean age, 71 years; range, 57–84) were compared with 17 younger subjects (mean age, 24 years; range, 20–36). The amplitude of the response in the elderly subjects in the visual cortex was significantly reduced relative to the younger individuals. However, the number of voxels activated was not significantly different between the young and the old (35). No effects of sex or cerebral atrophy were noted. In our study, we did not look at amplitude of response; we looked at the volume of activated brain. Ross's study suggests that elderly subjects do not necessarily show a reduced number of activated voxels solely on the basis of their age (given a reasonable threshold for activation). Thus, our findings of a reduced volume of activation need not be ascribed merely to generalized depression of function in the aged. Atrophy in the aged does not necessarily correspond to depression of the amplitude or volume of functional MR imaging activation (35). In the PET literature there are suggestions that global cerebral glucose utilization may be independent of brain size and age as well (36).

Our results are consistent with earlier functional MR imaging findings that the right frontal lobe is intimately associated with olfaction (1, 4). The right frontal lobe showed more voxels activated than the left at ratios from 2.39:1 to 8.0:1. These findings at functional MR imaging corroborate the PET literature, in which right frontal dominance as measured by cerebral blood flow with the $H2O^{15}$ technique has also been demonstrated during olfactory stimulation (37). Zatorre et al (37) have also demonstrated bilateral temporal lobe blood flow in-

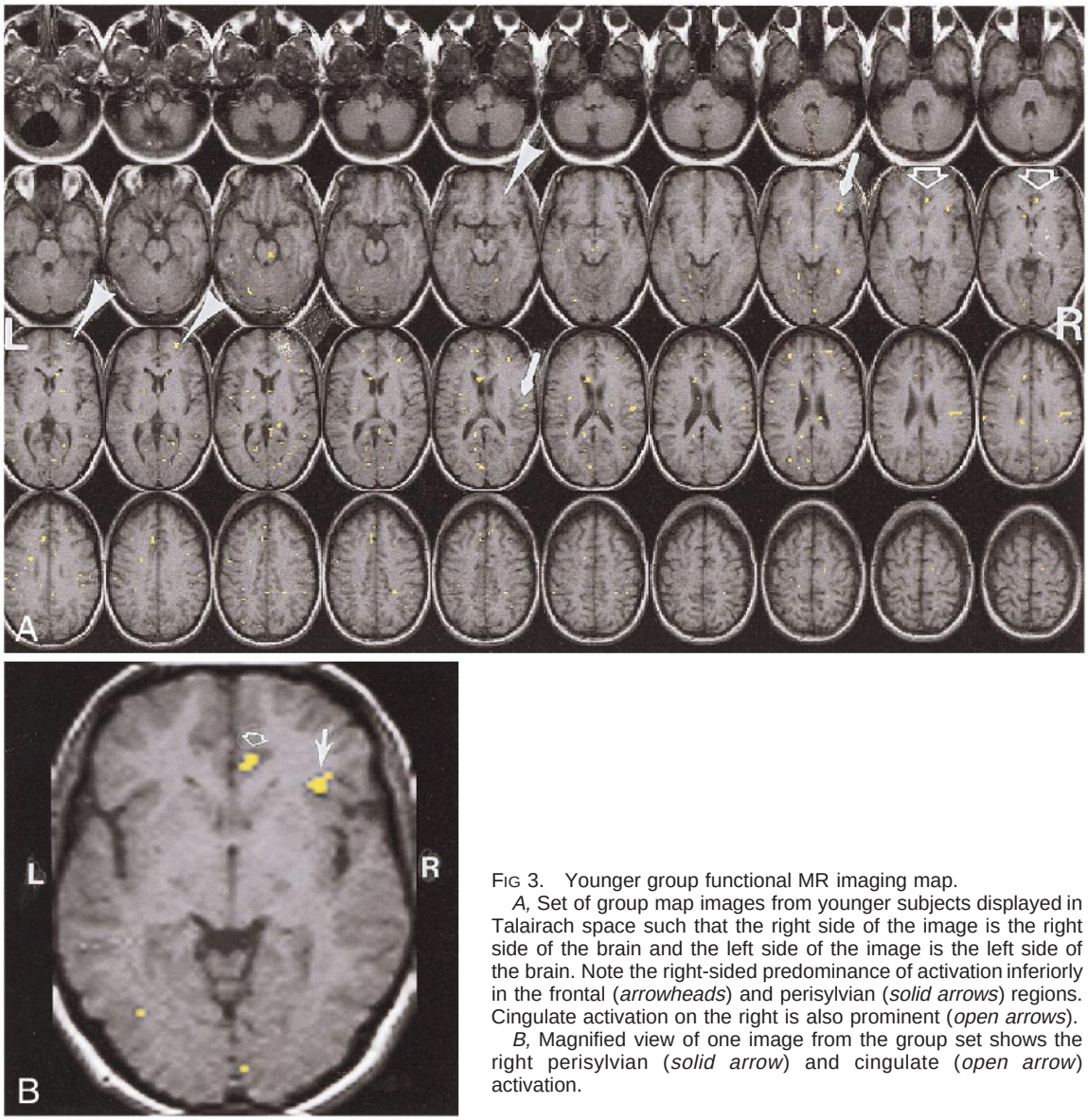

FIG 3. Younger group functional MR imaging map.

A, Set of group map images from younger subjects displayed in Talairach space such that the right side of the image is the right side of the brain and the left side of the image is the left side of the brain. Note the right-sided predominance of activation inferiorly in the frontal (*arrowheads*) and perisylvian (*solid arrows*) regions. Cingulate activation on the right is also prominent (*open arrows*).

B, Magnified view of one image from the group set shows the right perisylvian (*solid arrow*) and cingulate (*open arrow*) activation.

creases with olfactory stimulation, particularly in the perisylvian and piriform cortex regions.

Activation was seen in the occipital and parietal regions in the younger subjects' group maps. This was noted in a previous study, in which mixed olfactory and trigeminal nerve stimulants were used (1). Because these areas have not previously been reported to be instrumental in specific olfactory tasks, we attributed their occurrence to visual stimulation ''leakage'' in the darkened room and/or to a more generalized sensory stimulation that may occur in the secondary somatosensory regions from air flow or tactile stimulation from the olfactometer. This type of parietal activation has been shown in a previous study involving visual stimulation (38, 39).

Age is known to have a strong influence on the results of psychophysical tests of olfaction (7–10). There is a progressive decline in ability to identify odors with age in subjects over 60 years old (7–10). The functional MR imaging correlate is a diminution in the volume of activation after the age of 60. In our study we demonstrated a diminution in the number of activated voxels in older subjects compared with younger subjects. However, on individual maps, a number of older subjects did show some activation in the ''olfactory eloquent'' regions that have been described previously (Table 3), in accord with the heterogeneity of age-related olfactory loss.

As a group, women perform better than men on the UPSIT and on odor threshold tests at all age deciles (7, 40). Women also have larger olfactory evoked potential amplitudes than men (41) and discriminate among odors more accurately and with greater assurance than men (40). For this reason it is important to control for sex when performing odor-stimulated functional MR imaging studies.

There are several valid criticisms of this study that temper the reliability of our results. The sample size is small. Pulsing odors the way we did to

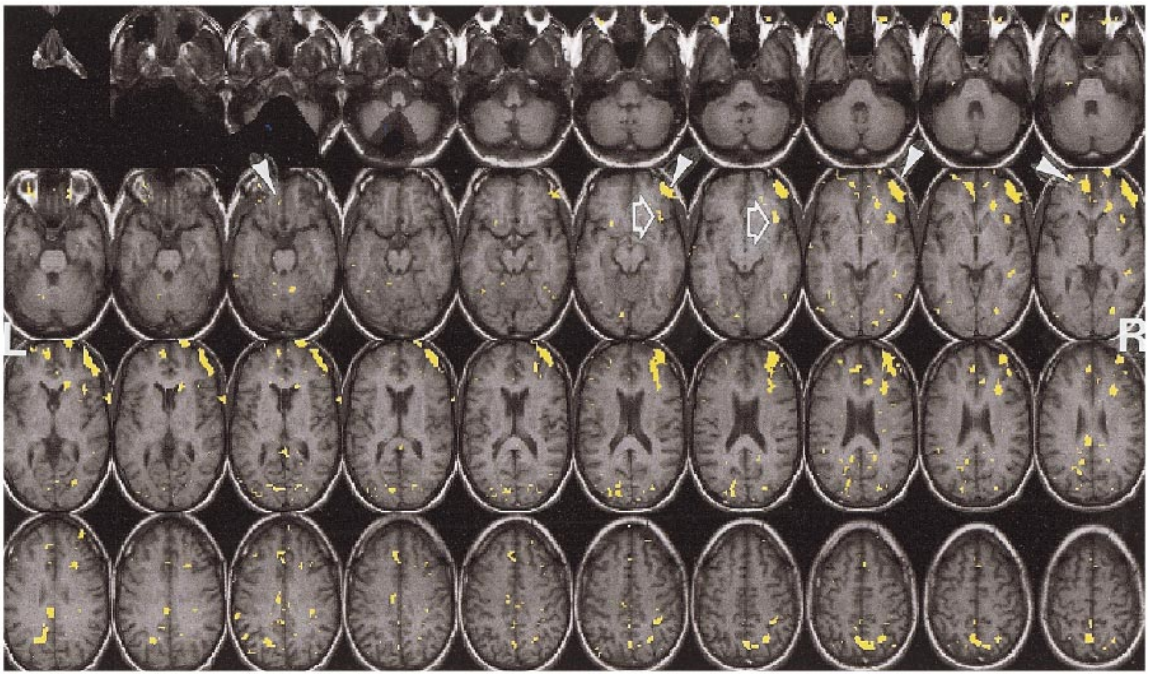

FIG 4. Activation map in single younger subject. Note the avid activation in both inferior frontal lobes (*arrowheads*), right more than left. Perisylvian activation inferiorly on the right (*open arrows*) is also noteworthy.

stimulate our subjects is not physiological, unless the analogy is that of a shopper at a perfume or cheese shop sniffing the products at regular intervals. While there may be some criticisms about the presence of volume loss in the brains associated with the elderly that could contribute to the diminution in activation in the older group, we believe that this can be addressed with the SPM analysis we performed. The SPM spatial normalization algorithms work by minimizing the difference of the sum of squares between the image that is to be normalized and a linear combination of one or more template images (25). A 12-parameter affine normalization is initially used to match the subject image to the reference template. This is followed by an elastic deformation computed in three dimensions. The elastic deformation works to correct for local variations in anatomy, and thus will correct for the effects of brain atrophy as well as for regional variation in the degree of atrophy.

We cannot separate the effects of diminution in cerebral blood flow in the elderly from the effects of decreased neuronal activation. A number of studies have shown differences in regional and global brain volumes in men and women of varying ages (42, 43). Fortunately, SPM96, by standardizing group-averaged brains to Talairach space, eliminates the issues of brain volume from analysis. The regional metabolism of the brain as measured by PET has also been shown to differ between men and women (30, 44). Men appear to have greater glucose utilization in the temporal lobes and cerebellum, whereas women have greater glucose utilization in the cingulate regions. Cerebral blood flow is also increased globally in women as compared with men (44). Is what we are seeing with odor-stimulated functional MR imaging a global reduction in activation in the older subjects? The articles by Grady et al (34) and Ross et al (35) suggest that one need not assume this is a global effect.

We also cannot control for any secondary thoughts or memories the odors may elicit in the magnet. However, the group maps are devised with the expectation that they correct for any individual's random thoughts. Finally, we must acknowledge that even with a reduction in TE to 30, there is significant susceptibility artifact at the skull base that can obscure activation. Coronal scanning may be better suited for these regions, but section limitations in the coronal plane obviate the ability to scan the whole brain (something that we could obtain in the axial plane). Nonetheless, the findings are clear that a difference between younger and older subjects exists on functional MR imaging maps of olfaction.

We believe that this work is a stepping stone to the screening of individuals at risk for developing Alzheimer disease (eg, with apolipoprotein-E karyotype E-4 or with early memory loss) or other neurodegenerative disorders that affect olfaction. Patients with Alzheimer disease have dramatic deficits in odor detection and identification (45–47). The deficits in olfactory identification are present in patients with early-stage Alzheimer disease and the deficits increase as the disease progresses (48, 49). Odor detection deficits appear later than identification deficits (48). Already, olfactory psychophysical tests have been able to identify a patient

population at risk for developing Alzheimer disease (50). We have also noted a near perfect correlation between the number of multiple sclerosis plaques in presumed ''olfactory eloquent'' regions and deficits on odor identification tests (51). As multiple sclerosis is the most common neurologic disease in the young and Alzheimer disease is one of the most common in the elderly, we believe that pursuing imaging tests of olfaction is critical in understanding neuropsychological pathogeneses. Olfactory-stimulated functional MR imaging may be able to detect brain deficits in patients with many of these neurologic diseases at an earlier stage, when pharmacologic intervention would likely be of greatest benefit.

Conclusion

Age may be a factor with regard to the results of odor-stimulated functional MR imaging studies. Whether this is a generalized effect that may be seen with all stimuli or is selective to the sense of smell remains to be investigated. In either case, when studying odor-stimulated functional MR imaging, the age of the subjects is a variable for which one must control.

References

1. Yousem DM, Williams SC, Howard RO, et al. **Functional MR imaging during odor stimulation: preliminary data.** *Radiology* 1997;204:833–838
2. Levy LM, Henkin RI, Hutter A, Lin CS, Martins D, Schellinger D. **Functional MRI of human olfaction.** *J Comput Assist Tomogr* 1997;21:849–856
3. Levy LM, Henkin RI, Hutter A, Lin CS, Schellinger D. **Mapping brain activation to odorants in patients with smell loss by functional MRI.** *J Comput Assist Tomogr* 1998;22:96–103
4. Koizuka I, Yano H, Nagahara M, et al. **Functional imaging of the human olfactory cortex by magnetic resonance imaging.** *ORL J Otorhinolaryngol Relat Spec* 1994;56:273–275
5. Kettenmann B, Jousmaki V, Portin K, Salmelin R, Kobal G, Hari R. **Odorants activate the human superior temporal sulcus.** *Neurosci Lett* 1996;203:143–145
6. Sobel N, Prabhakaran V, Hartley CA, et al. **Odorant-induced and sniff-induced activation in the cerebellum of the human.** *J Neurosci* 1998;18:8990–9001
7. Doty RL. **Influence of age and age-related diseases on olfactory function.** *Ann N Y Acad Sci* 1989;561:76–86
8. Doty RL, Applebaum S, Zusho H, Settle RG. **Sex differences in odor identification ability: a cross-cultural analysis.** *Neuropsychologia* 1985;23:667–672
9. Doty RL, Brugger WE, Jurs PC, Orndorff MA, Snyder PJ, Lowry LD. **Intranasal trigeminal stimulation from odorous volatiles: psychometric responses from anosmic and normal humans.** *Physiol Behav* 1978;20:175–185
10. Deems DA, Doty RL. **Age-related changes in the phenyl ethyl alcohol odor detection threshold.** *Trans Penn Acad Ophthalmol Otolaryngol* 1987;39:646–650
11. Doty RL, Shaman P, Kimmelman CP, Dann MS. **University of Pennsylvania Smell Identification Test: a rapid quantitative olfactory function test for the clinic.** *Laryngoscope* 1984;94: 176–178
12. Doty RL, Shaman P, Dann M. **Development of the University of Pennsylvania Smell Identification Test: a standardized microencapsulated test of olfactory function.** *Physiol Behav* 1984; 32:489–502
13. Doty RL, Shaman P, Applebaum SL, Giberson R, Siksorski L, Rosenberg L. **Smell identification ability: changes with age.** *Science* 1984;226:1441–1443
14. Kopala LC, Good K, Honer WG. **Olfactory identification ability in pre- and postmenopausal women with schizophrenia.** *Biol Psychiatry* 1995;38:57–63
15. Murphy C. **Cognitive and chemosensory influences on age-related changes in the ability to identify blended foods.** *J Gerontol* 1985;40:47–52
16. Murphy C. **Age-related effects on the threshold, psychophysical function, and pleasantness of menthol.** *J Gerontol* 1983; 38:217–222
17. Briggs GG, Nebes RD. **Patterns of hand preference in a student population.** *Cortex* 1975;11:230–238
18. Deems DA, Doty RL, Settle RG, et al. **Smell and taste disorders: a study of 750 patients from the University of Pennsylvania Smell and Taste Center.** *Arch Otolaryngol Head Neck Surg* 1991;117:519–528
19. Hummel T, Pietsch H, Kobal G. **Kallmann's syndrome and chemosensory evoked potentials.** *Eur Arch Otorhinolaryngol* 1991;248:311–312
20. Kobal G, Hummel C. **Cerebral chemosensory evoked potentials elicited by chemical stimulation of the human olfactory and respiratory nasal mucosa.** *Electroencephalogr Clin Neurophysiol* 1988;71:241–250
21. Sobel N, Prabhakaran V, Desmond JE, et al. **Sniffing and smelling: separate subsystems in the human olfactory cortex.** *Nature* 1998;392:282–286
22. Friston KJ, Frith CD, Liddle PF, Frackowiak RS. **Comparing functional (PET) images: the assessment of significant change.** *J Cereb Blood Flow Metab* 1991;11:690–699
23. Friston KJ, Worsley KJ, Frackowiak RSJ, Mazziotta JC, Evans AC. **Assessing the significance of focal activations using their spatial extent.** *Hum Brain Map* 1994;1:214–220
24. Friston KJ. **Commentary and opinion, II: statistical parametric mapping: ontology and current issues.** *J Cereb Blood Flow Metab* 1995;15:361–370
25. Friston K, Holmes A, Worsley K, Poline J, Frith C, Frackowiak R. **Statistical parametric maps in functional imaging: a general approach.** *Hum Brain Map* 1995;2:189–201
26. Friston K, Ahburner J, Poline J, Frith C, Heather J, Frackowiak R. **Spatial realignment and normalization of images.** *Hum Brain Map* 1995;2:202–214
27. Friston KJ, Frith CD, Liddle PF, Dolan RJ, Lammertsma AA, Frackowiak RS. **The relationship between global and local changes in PET scans [see comments].** *J Cereb Blood Flow Metab* 1990;10:458–466
28. Levin JM, Ross MH, Mendelson JH, Mello NK, Cohen BM, Renshaw PF. **Sex differences in blood-oxygenation-level-dependent functional MRI with primary visual stimulation.** *Am J Psychiatry* 1998;155:434–436
29. Gur RC, Gur RE, Obrist WD, et al. **Sex and handedness differences in cerebral blood flow during rest and cognitive activity.** *Science* 1982;217:659–661
30. Gur RC, Mozley LH, Mozley PD, et al. **Sex differences in regional cerebral glucose metabolism during a resting state.** *Science* 1995;267:528–531
31. Andreason PJ, Zametkin AJ, Guo AC, Baldwin P, Cohen RM. **Gender-related differences in regional cerebral glucose metabolism in normal volunteers.** *Psychiatry Res* 1994;51:175–183
32. Miura SA, Schapiro MB, Grady CL, et al. **Effect of gender on glucose utilization rates in healthy humans: a positron emission tomography study.** *J Neurosci Res* 1990;27:500–504
33. Azari NP, Rapoport SI, Salerno JA, et al. **Interregional correlations of resting cerebral glucose metabolism in old and young women.** *Brain Res* 1992;589:279–290
34. Grady CL, Maisog JM, Horwitz B, et al. **Age-related changes in cortical blood flow activation during visual processing of faces and location.** *J Neurosci* 1994;14:1450–1462
35. Ross MH, Yurgelun-Todd DA, Renshaw PF, et al. **Age-related reduction in functional MRI response to photic stimulation.** *Neurology* 1997;48:173–176
36. Hatazawa J, Brooks RA, Di Chiro G, Campbell G. **Global cerebral glucose utilization is independent of brain size: a PET study.** *J Comput Assist Tomogr* 1987;11:571–576
37. Zatorre RJ, Jones-Gotman M, Evans AC, Meyer E. **Functional localization and lateralization of human olfactory cortex.** *Nature* 1992;360:339–340
38. Kraut MA, Marenco S, Soher BJ, Wong DF, Bryan RN. **Comparison of functional MR and H2 15O positron emission tomography in stimulation of the primary visual cortex.** *AJNR Am J Neuroradiol* 1995;16:2101–2107

39. Kraut M, Hart J Jr, Soher BJ, Gordon B. **Object shape processing in the visual system evaluated using functional MRI.** *Neurology* 1997;48:1416–1420
40. Gilbert AN, Greenberg MS, Beauchamp GK. **Sex, handedness and side of nose modulate human odor perception [published erratum appears in *Neuropsychologia* 1989;27:1313].** *Neuropsychologia* 1989;27:505–511
41. Evans WJ, Cui L, Starr A. **Olfactory event-related potentials in normal human subjects: effects of age and gender.** *Electroencephalogr Clin Neurophysiol* 1995;95:293–301
42. Cowell PE, Turetsky BI, Gur RC, Grossman RI, Shtasel DL, Gur RE. **Sex differences in aging of the human frontal and temporal lobes.** *J Neurosci* 1994;14:4748–4755
43. Gur RC, Mozley PD, Resnick SM, et al. **Gender differences in age effect on brain atrophy measured by magnetic resonance imaging.** *Proc Natl Acad Sci U S A* 1991;88:2845–2849
44. Gur RE, Gur RC. **Gender differences in regional cerebral blood flow.** *Schizophrenia Bull* 1990;16:247–254
45. Doty RL, Reyes PF, Gregor T. **Presence of both odor identification and detection deficits in Alzheimer's disease.** *Brain Res Bull* 1987;18:597–600
46. Doty RL. **Olfactory capacities in aging and Alzheimer's disease: psychophysical and anatomic considerations.** *Ann NY Acad Sci* 1991;640:20–27
47. Doty RL, Perl DP, Steele JC, et al. **Olfactory dysfunction in three neurodegenerative diseases.** *Geriatrics* 1991;46:47–51
48. Serby M, Larson P, Kalkstein D. **The nature and course of olfactory deficits in Alzheimer's disease.** *Am J Psychiatry* 1991; 148:357–360
49. Rezek DL. **Olfactory deficits as a neurologic sign in dementia of the Alzheimer type.** *Arch Neurol* 1987;44:1030–1032
50. Bacon AW, Hartwell V, Quinones R, et al. **The role of apolipoprotein-E and olfactory functioning in people with Alzheimer's disease.** Presented at the International Symposium on Smell and Taste, San Diego, 1997
51. Doty RL, Li C, Mannon LJ, Yousem DM. **Olfactory dysfunction in multiple sclerosis [letter].** *N Engl J Med* 1997;336:1918–1919